

THEME A

Formulator: ENEL/HYDRO – Polo Idraulico e Strutturale

Evaluation of AAR (Alkali – Aggregate Reaction) effects on the structural behaviour of an arch dam: interpretation of the measured behaviour and forecasting of the future trend

E. Bon, F. Chille, P. Masarati, C. Massaro

Analysis of the effects induced by alkali-aggregate reaction (AAR) on the structural behavior of Pian Telesio dam

A. Popovici, R. Sarghiuta, A. Abdulamit, C. Ilinca

Forecast on stress-strain state generated by Alkali-Aggregate Reaction (AAR) from Pian Telesio Dam

Formulator: ENEL/HYDRO – Polo Idraulico e Strutturale
Evaluation of AAR (Alkali – Aggregate Reaction) effects on the structural behaviour of an arch dam: interpretation of the measured behaviour and forecasting of the future trend



INTERNATIONAL COMMISSION ON LARGE DAMS

Ad Hoc Committee on Computational Aspects of Analysis and Design of Dams

COMMISSION INTERNATIONALE DES GRANDS BARRAGES

Comité Ad Hoc des Méthodes de Calculs pour Barrages

6th INTERNATIONAL BENCHMARK WORKSHOP
ON NUMERICAL ANALYSIS OF DAMS

October 17-19, 2001, Salzburg - Austria

Theme A - Concrete dams

Evaluation of AAR (Alkali - Aggregate Reaction)

effects on the structural behaviour of an arch dam:

interpretation of the measured behaviour and forecasting of the future trend



1 INTRODUCTION

1.1 Objective of this Benchmark

Theme A concerns the analysis of the measurement results for the horizontal crest displacements of Pian Telessio Arch-Gravity Dam (Italy). The dam monitoring data (measurements carried out by means of collimators, plumb-lines, inclinometers, thermometers, etc.), integrated with laboratory test data on AAR phenomenon which affects the structure, will be used to perform a back-analysis for a model calibration in order to evaluate the present and the future stress-strain state.

1.2 General Information about Pian Telessio Dam

1.2.1 Description of Dam

Pian Telessio dam is an arch-gravity structure located in the North-West of Italy in the Piemonte region. The dam owner is the A.E.M. of Turin, a municipal electric company. The construction of the dam was completed in 1956 and it came into operation in 1958. The most important data are here below summarized:

- max height 80 m
- crest length 515 m
- crest elevation 1919 m a.s.l.
- max storage level 1917 m a.s.l.
- reservoir volume 23.5 Mm³

In Fig. 1 a picture of the dam is shown. Fig. 2 shows the main cross section of the structure: the presence of the pulvino can be observed as well as the shafts for plumb-lines.

1.2.2 Instrumentation

Fig. 3 shows the position of the most important instruments installed on the dam:

- plumb-lines located on 4 vertical sections
- collimators on the dam crest
- extensometers on joints

Four measurement stations are located along each plumb-line, according to the scheme reported in fig. 4.

1.2.3 Observed behaviour

For a long period, from the end of the construction to the middle of '70s, the dam has shown a very normal behaviour, well correlated with the variations of the environmental conditions (storage level and ambient temperatures).



Soon after, the measurements have shown a marked upstream drift with some discontinuities during period in which the average storage level. This behaviour has been also confirmed by the collimators and the inclinometers.

1.2.4 *Detection of the problem*

When the upstream drift was observed, additional and/or more frequent measurements and investigations were carried out in order to reach a sound explanation of the phenomena.

In the last years, among others, physical-chemical analyses on concrete have been carried out. These investigations have clearly shown the presence of the well know AAR (Alkali-Aggregate Reaction) phenomenon, due to aggregates mainly composed by gneiss, micaschists and quartz and also to a high alkali content in the cement adopted for the concrete mix.

Accelerated tests carried out on mortar specimens prepared with the same aggregates have confirmed the slow-moderate activity of the reaction, even if the lack of specific tests does not allow to directly quantify its velocity in terms of $\mu\text{m}/\text{m}/\text{year}$.

2 ANALYSIS DATA

2.1 *Monitoring Data*

Water level, daily mean air temperature, plumbines displacements, whose plots are reported in Figs. 5÷7, are provided with Excel file *measurements.xls*.

2.2 *F.E. model Data*

2.2.1 *F.E. mesh*

The FE Mesh of dam-foundation system, including peripheral joint (Fig. 8), is composed by 10472 nodes and 2044 elements. The mesh data are contained in the following files:

NODES.TXT node labels, x-, y-, z-coordinates: 10472 records, format '(i6,3(1pe16.8))'
FOU20.TXT foundation parabolic brick elements topology: 1320 records, format '21i5'
PUL20.TXT pulvino parabolic brick elements topology: 112 records, format '21i5'
DAM20.TXT dam parabolic brick elements topology: 464 records, format '21i5'
DAM15.TXT dam parabolic wedge elements topology: 48 records, format '16i5'
INT16.TXT peripheral joint parabolic quadrilateral interface elements topology: 100 records, format '17i5'

Element topologies are defined according to the numbering conventions indicated in fig. 9.



2.2.2 Material parameters

Elastic parameters for both dam concrete and foundation rock are defined in the following table:

	<i>Young Modulus E</i>	<i>Poisson Ratio ν</i>	<i>density ρ</i>
<i>Dam</i>	20000 MPa	0.2	2450 Kgm/mc
<i>Foundation</i>	28000 MPa	0.2	0.

The following constitutive law is proposed for the joint behaviour description: perfectly unilateral in normal direction; elastic in shear direction (no additional parameter needed in this case).

Participants are allowed to adopt more sophisticated material constitutive laws, provided that assumptions on missing parameters have to be made in order to fulfill the lack of information in data provided herein.

2.2.3 Loads

The following loads have to be considered: dead weight, hydrostatic pressure according to reservoir level at maximum storage level (1917 m a.s.l.) and volumetric strain due to AAR.

The latter can be expressed according to the following general expression:

$$\varepsilon = \varepsilon (t, X, \sigma, p_1, \dots, p_n)$$

where t represents the time, X the generic dam point location; σ the stress tensor; $p_1 \dots p_n$ any other significant physical parameter (i.e. moisture content, temperature, etc.). Data provided herein are sufficient to properly define the BW theme A exercise when the following simple law is assumed:

$$\varepsilon = k t$$

where k is a constant value to be identified on the basis of observed crest up-downstream displacement.

Participants are allowed to adopt more sophisticated laws, provided that assumptions on missing parameters have to be made in order to fulfill the lack of information in data provided herein. In particular for those participants who intend relate volumetric strain to the local stress state, it is important to properly consider the thermal load effects. In this connection additional data referring to air and water temperatures are provided with Excel file *measurements.xls*.

3 REQUIRED OUTPUT

- Displacements vs. time for the period 1970÷2020, at nodes 1÷7 indicated in Fig. 10 and listed in file NOUT.TXT (7 nodes).



- Principal minimum, intermediate, maximum stresses at time 1999 and 2020, at nodes belonging to upstream and downstream faces and the vertical cross-section highlighted in Fig. 10; the relevant node label lists are contained in the files NUPSTR.TXT (560 nodes), NDOWNSTR.TXT (560 nodes), NSECTION.TXT (158 nodes).

Participants can provide additional output results relevant to the most peculiar and significant aspects typically related to the adopted solution procedures.



Fig. 1- Pian Telesio Dam

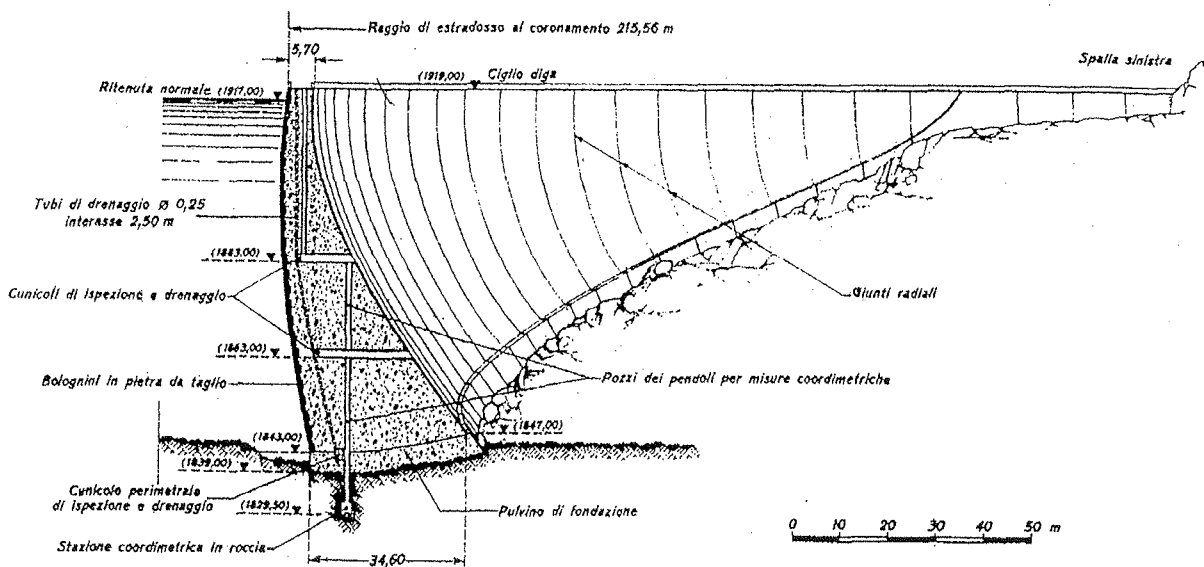


Fig. 2- Main cross section of the dam

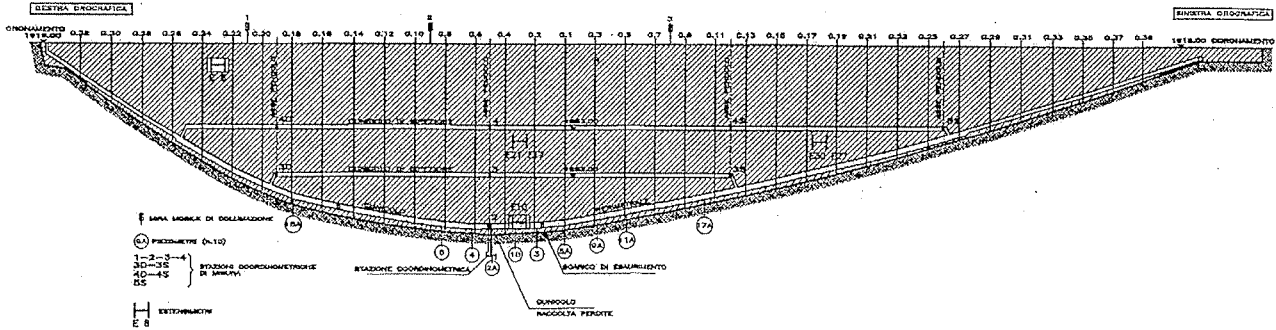


Fig. 3- Position of the most important instruments installed on the dam

Fig. 4- Measurement stations locations along each plumbline

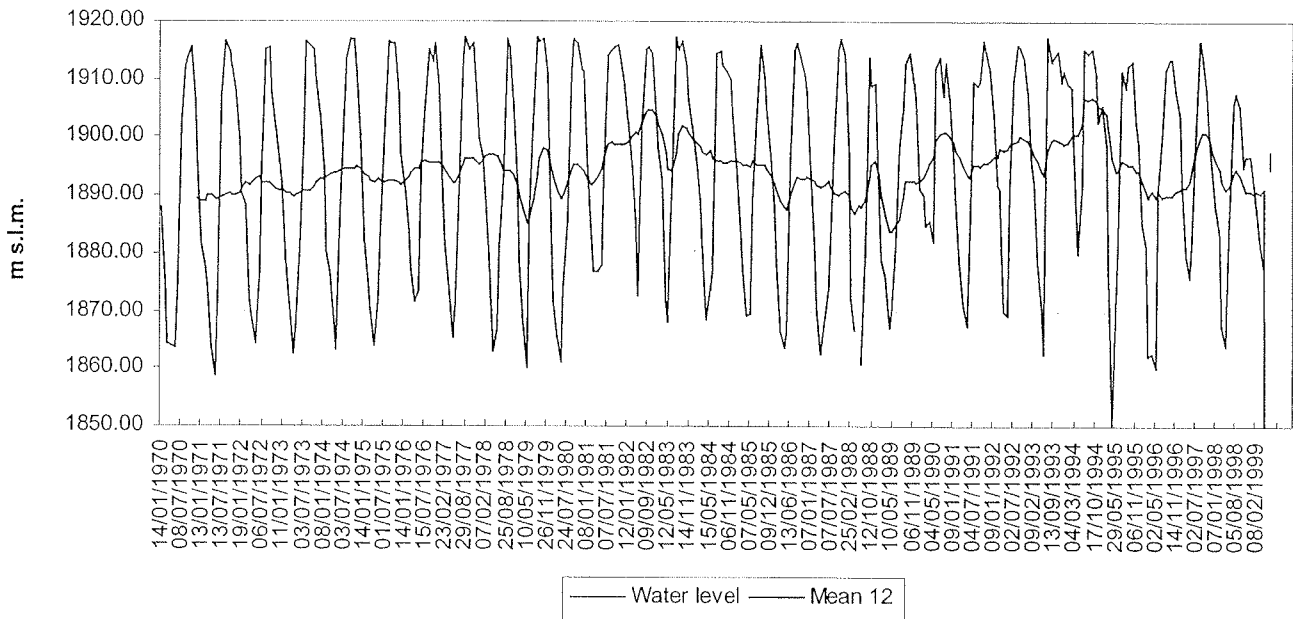


Fig. 5- Water level time history

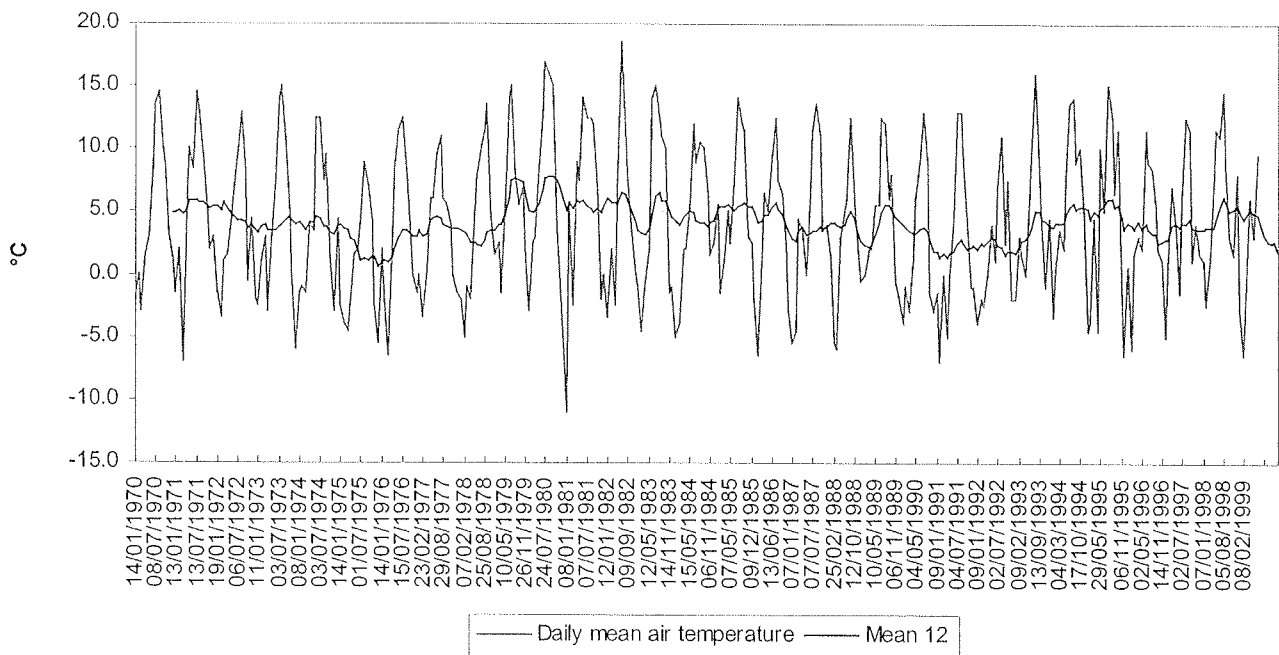


Fig. 6- Daily mean air temperature time history



Central Plumblines (concio 4/6)

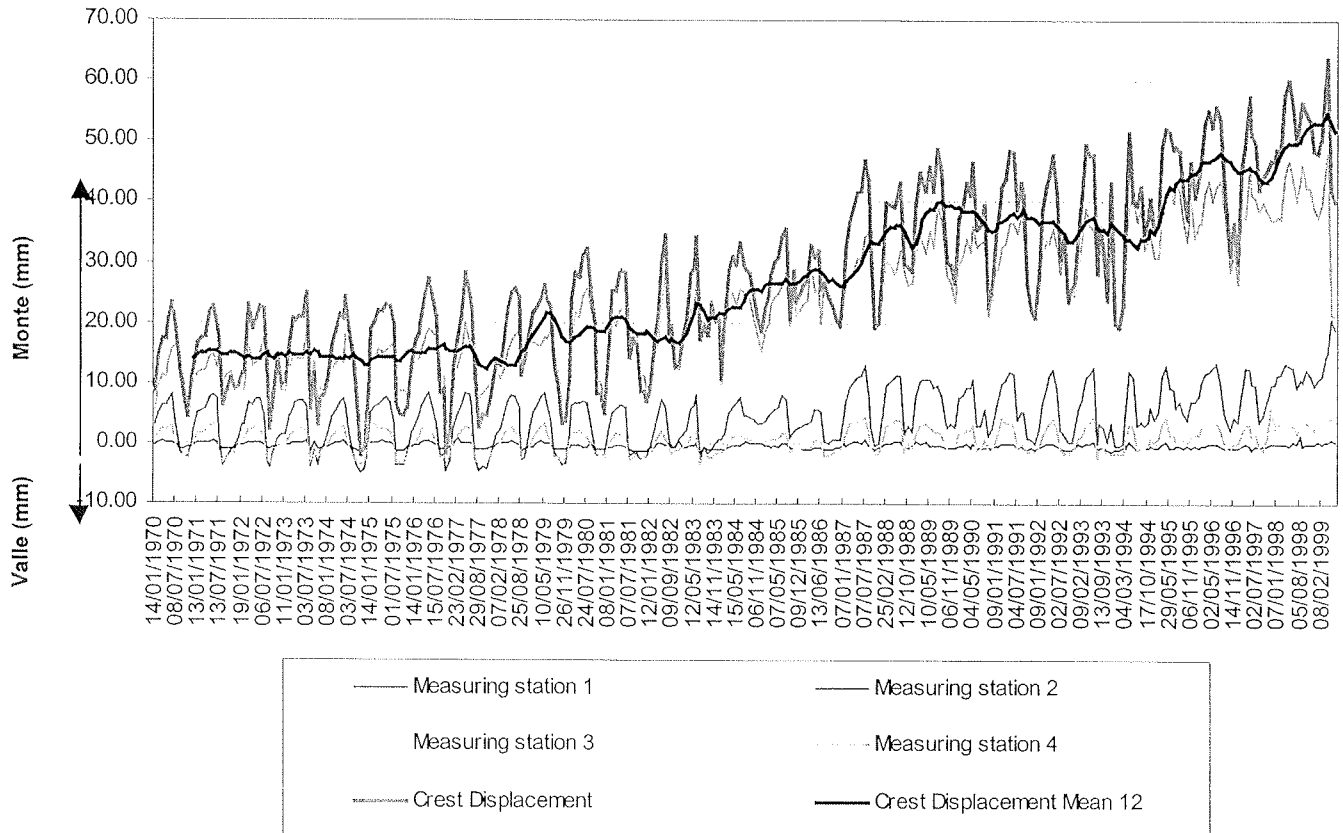


Fig. 7- Upstream-downstream central plumblines and crest displacement time histories

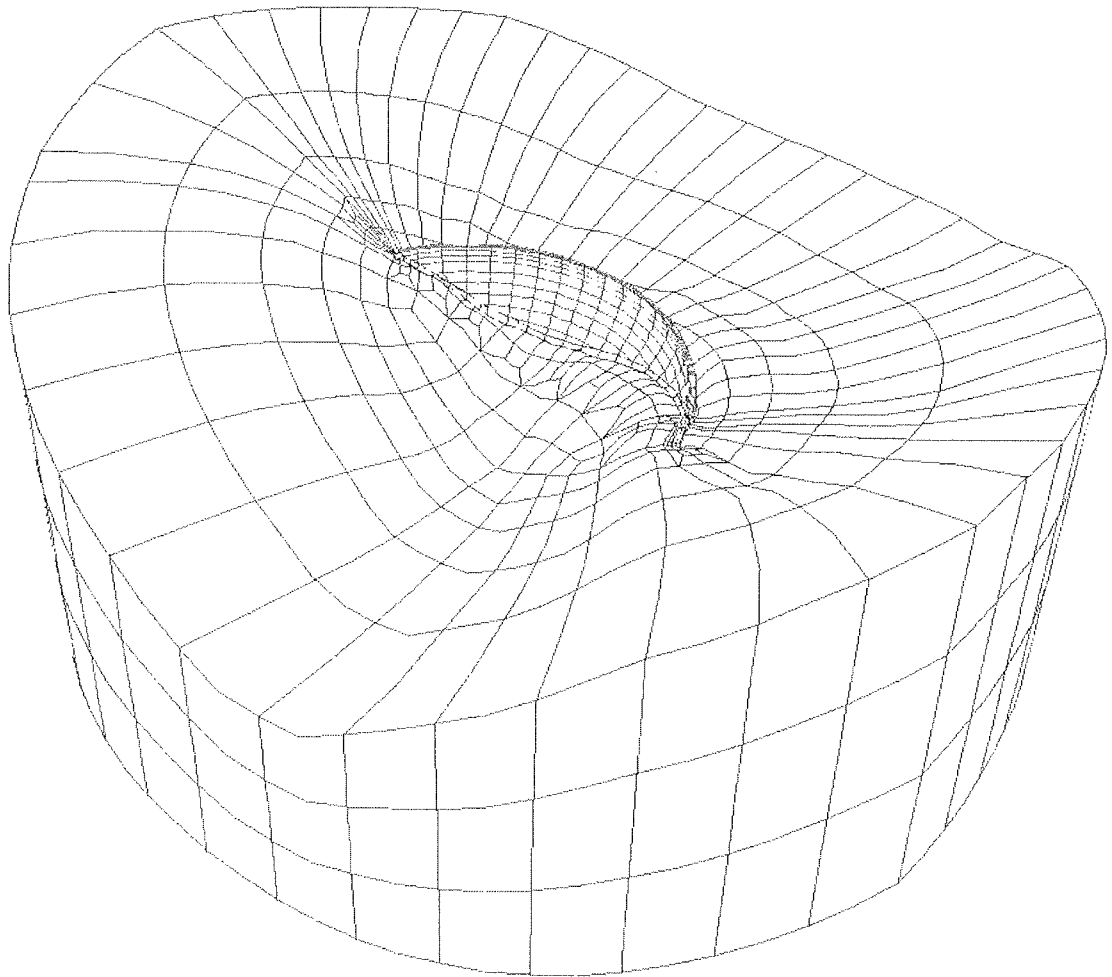


Fig. 8- Finite Element Mesh

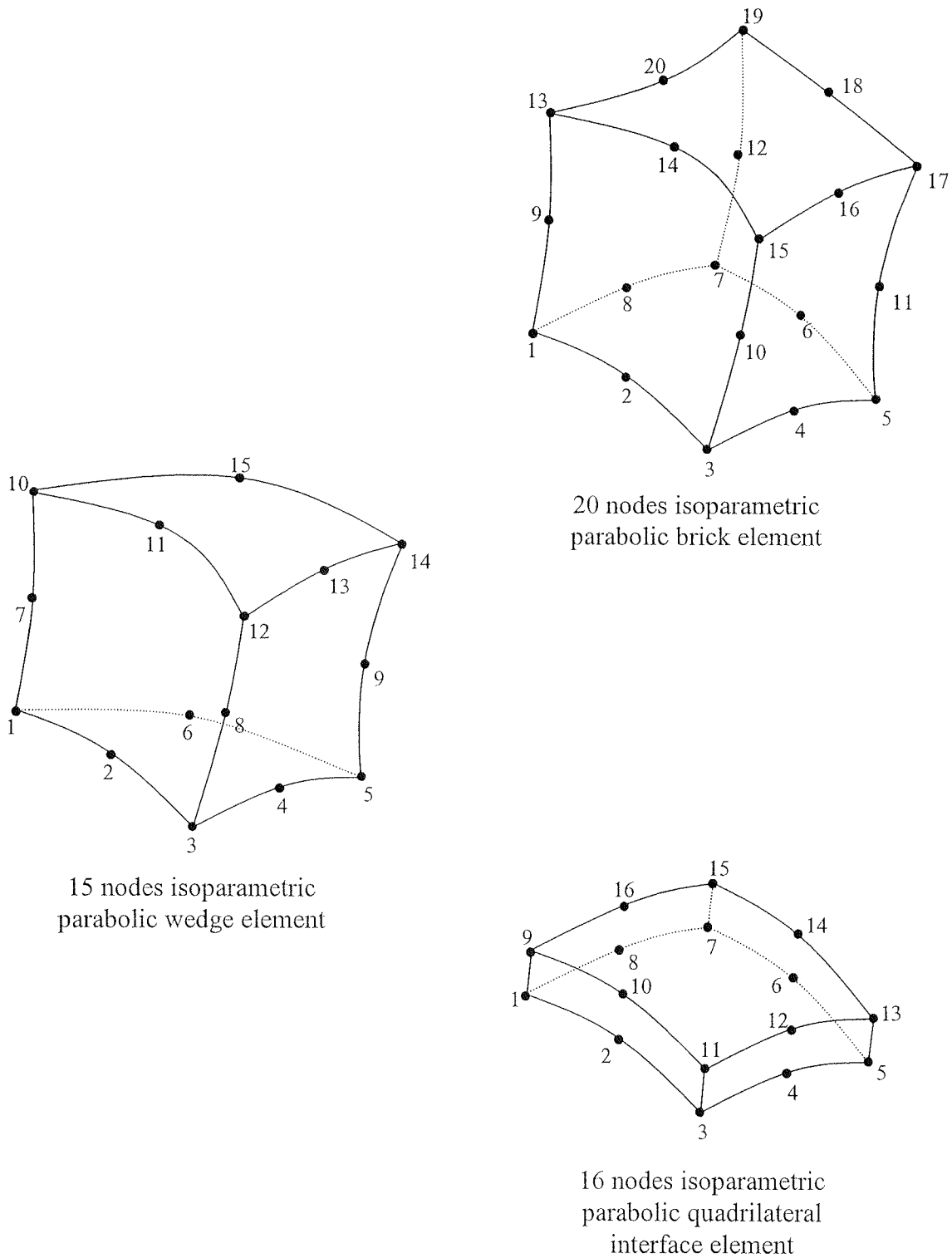


Fig. 9- Numbering convention adopted for each used element type

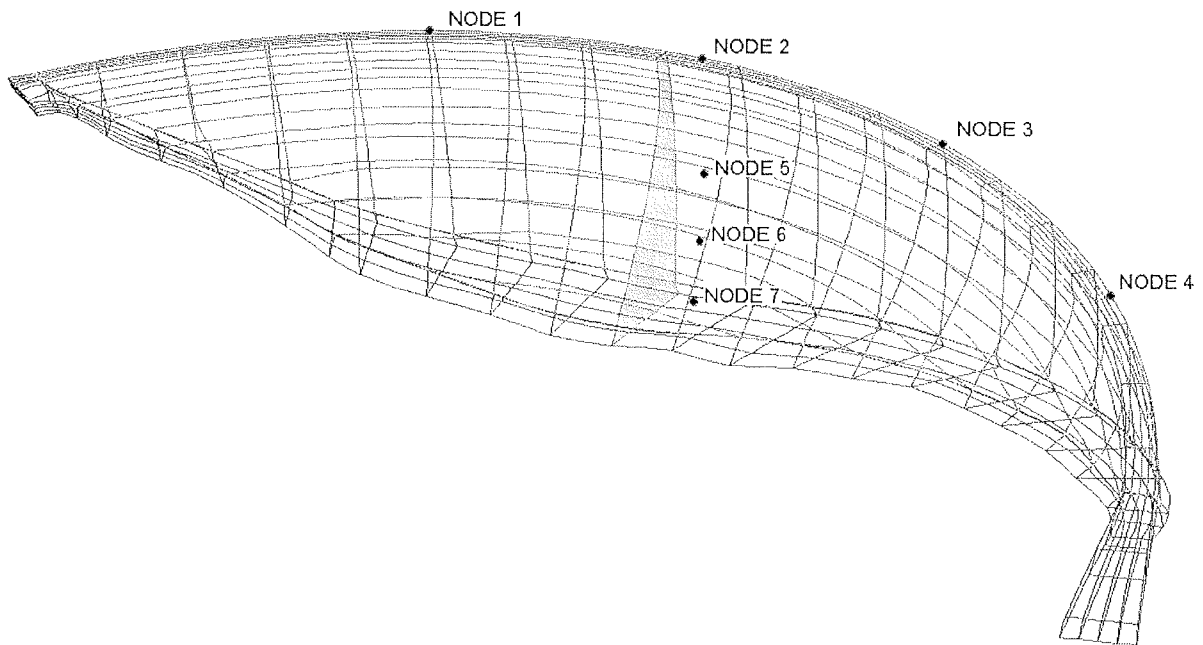
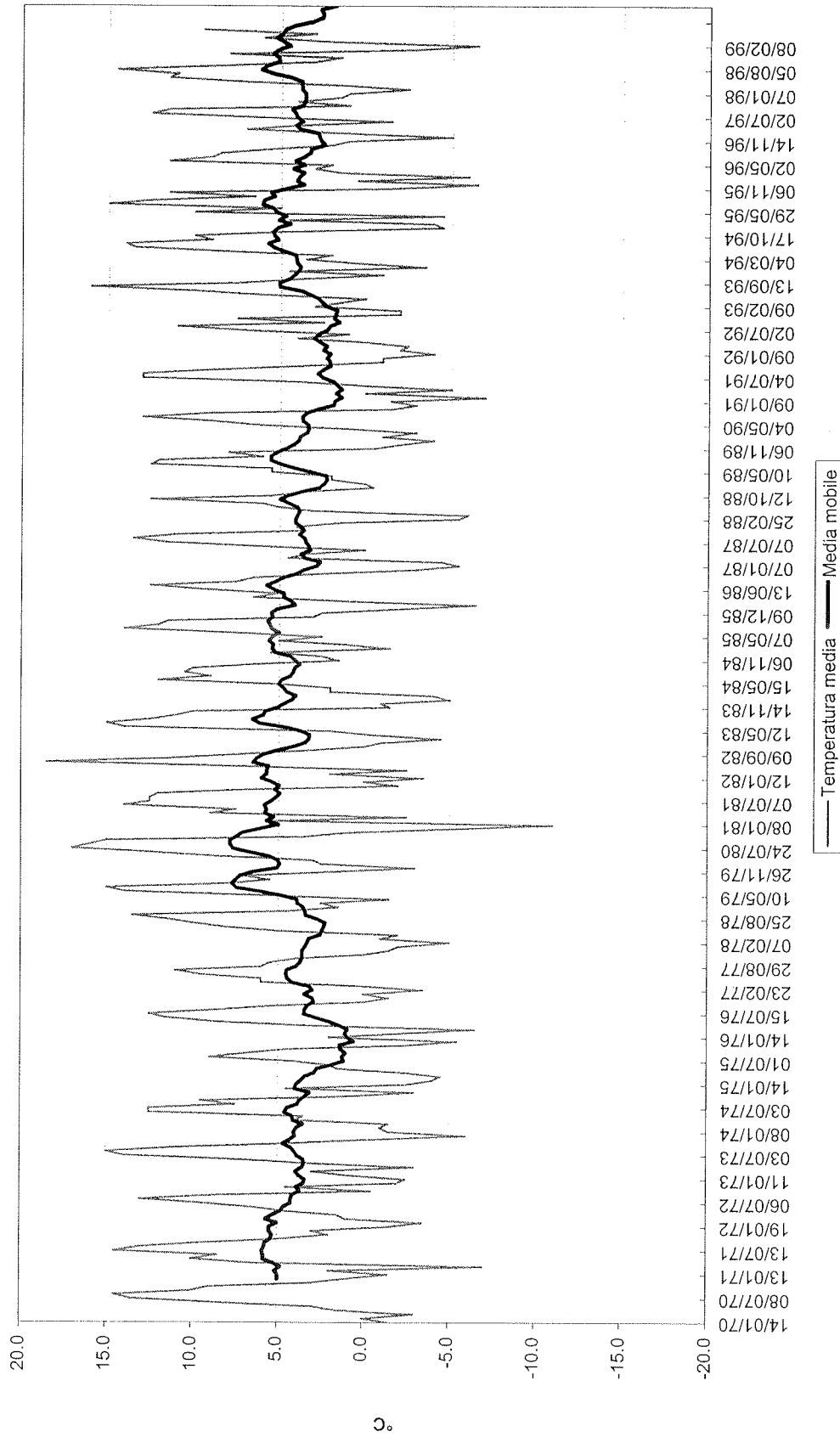


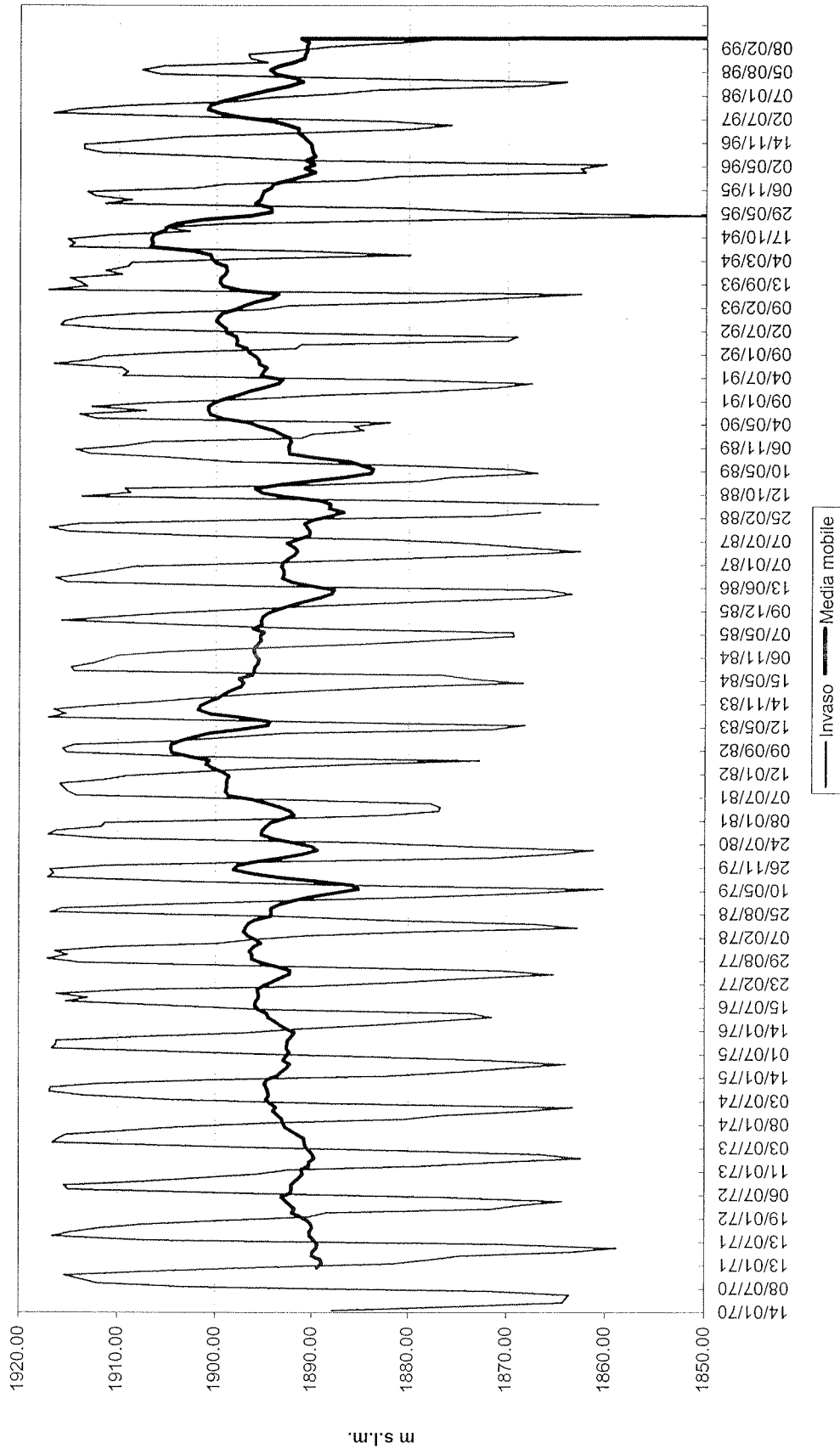
Fig. 10- Location of output selected nodes and central vertical section

Diga Pianteleccio

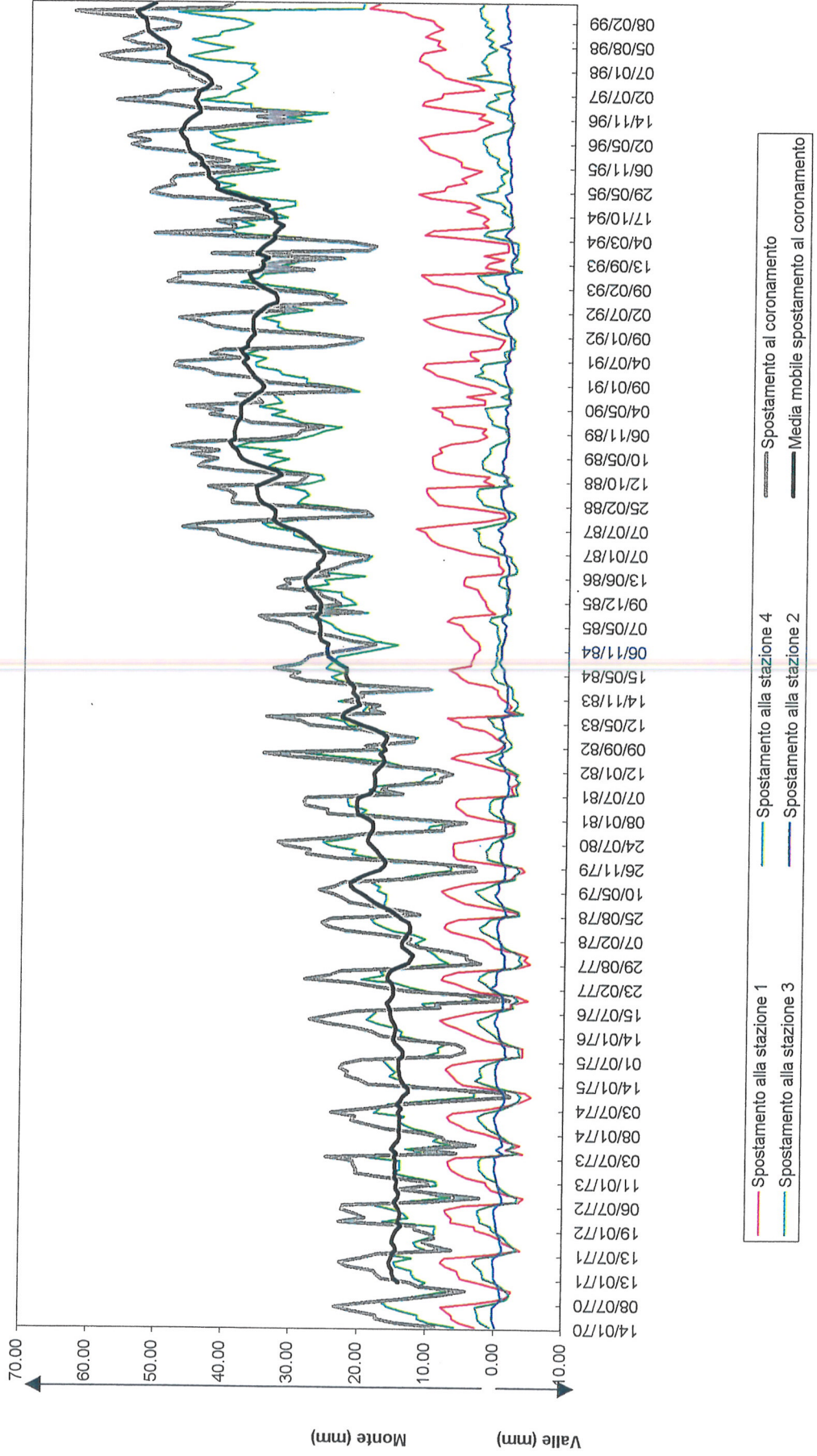
Temperatura media



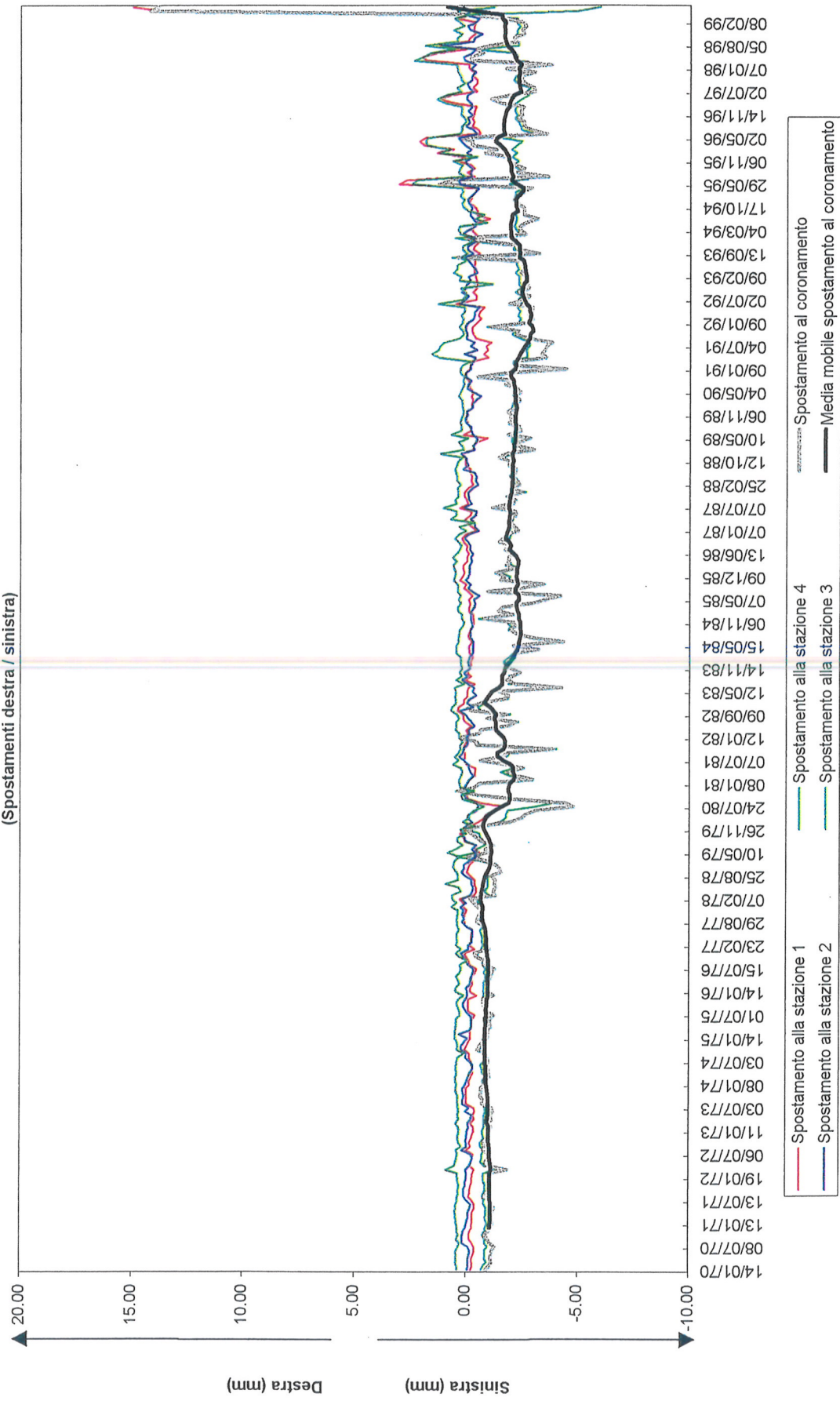
Diga Pianteleccio Invaso



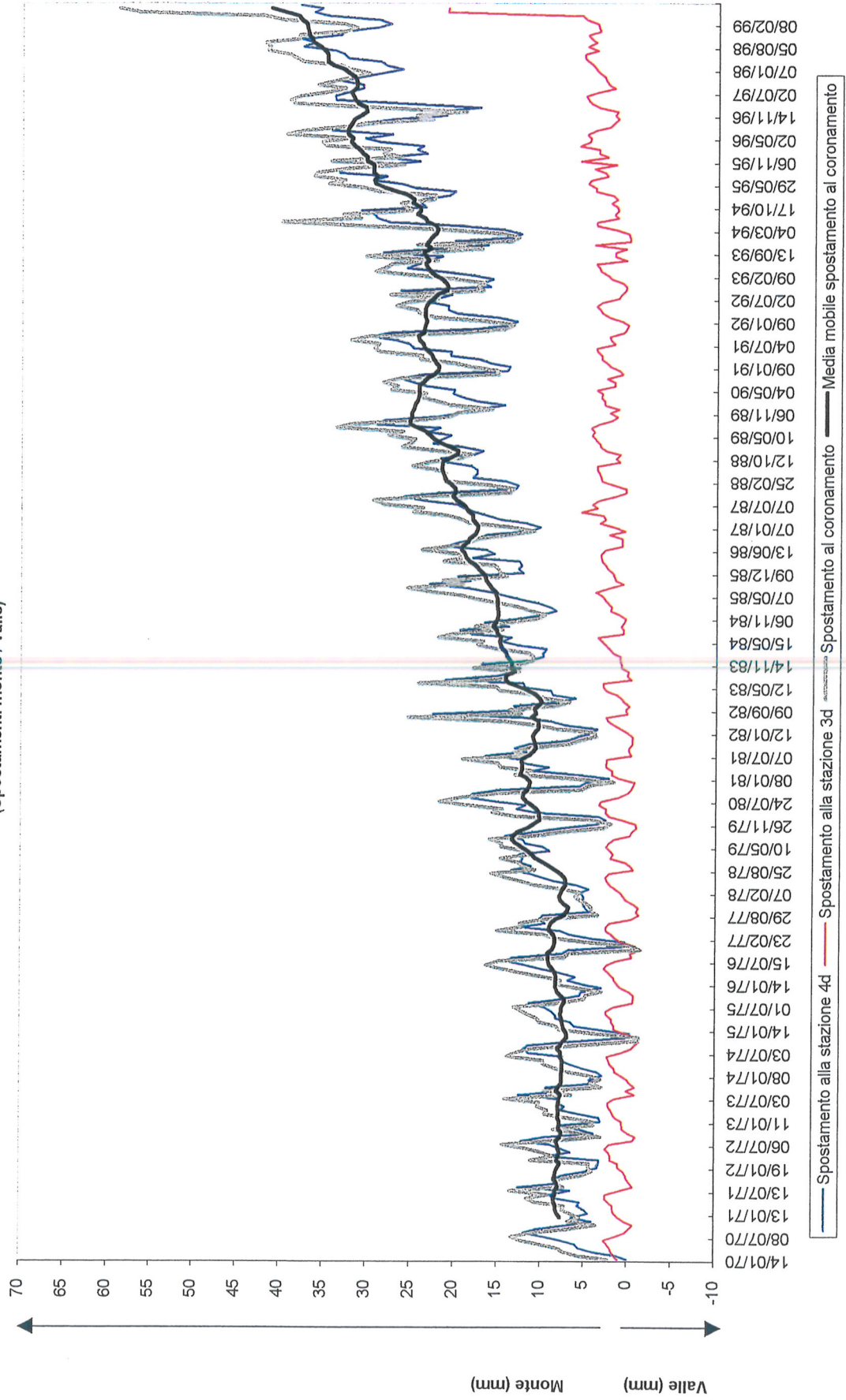
Diga Pianteleccio
Pendolo centrale (concio 4/6)
(Spostamenti monte / valle)



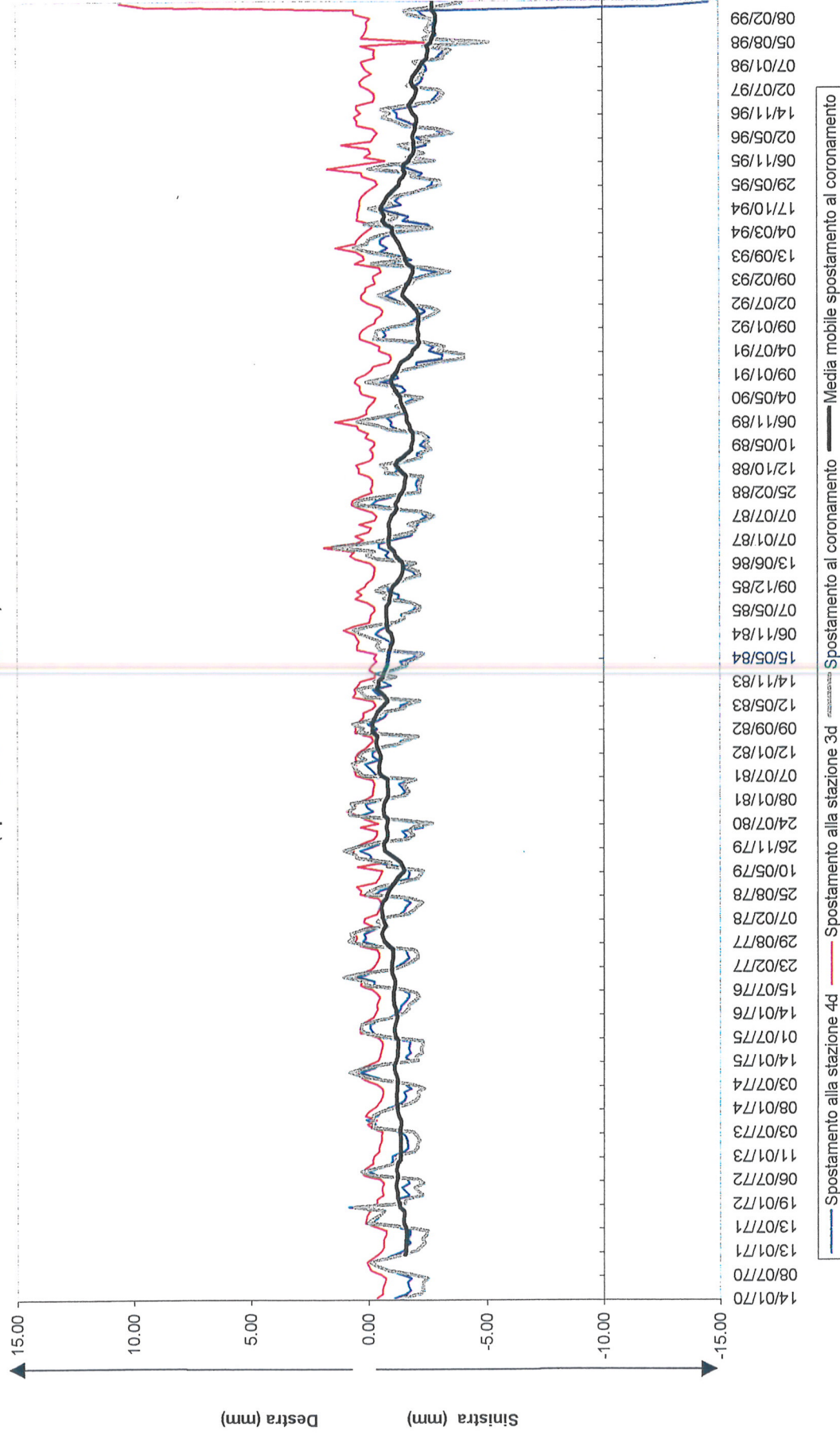
Diga Pianteleccio
Pendolo centrale (concio 4/6)
(Spostamenti destra / sinistra)



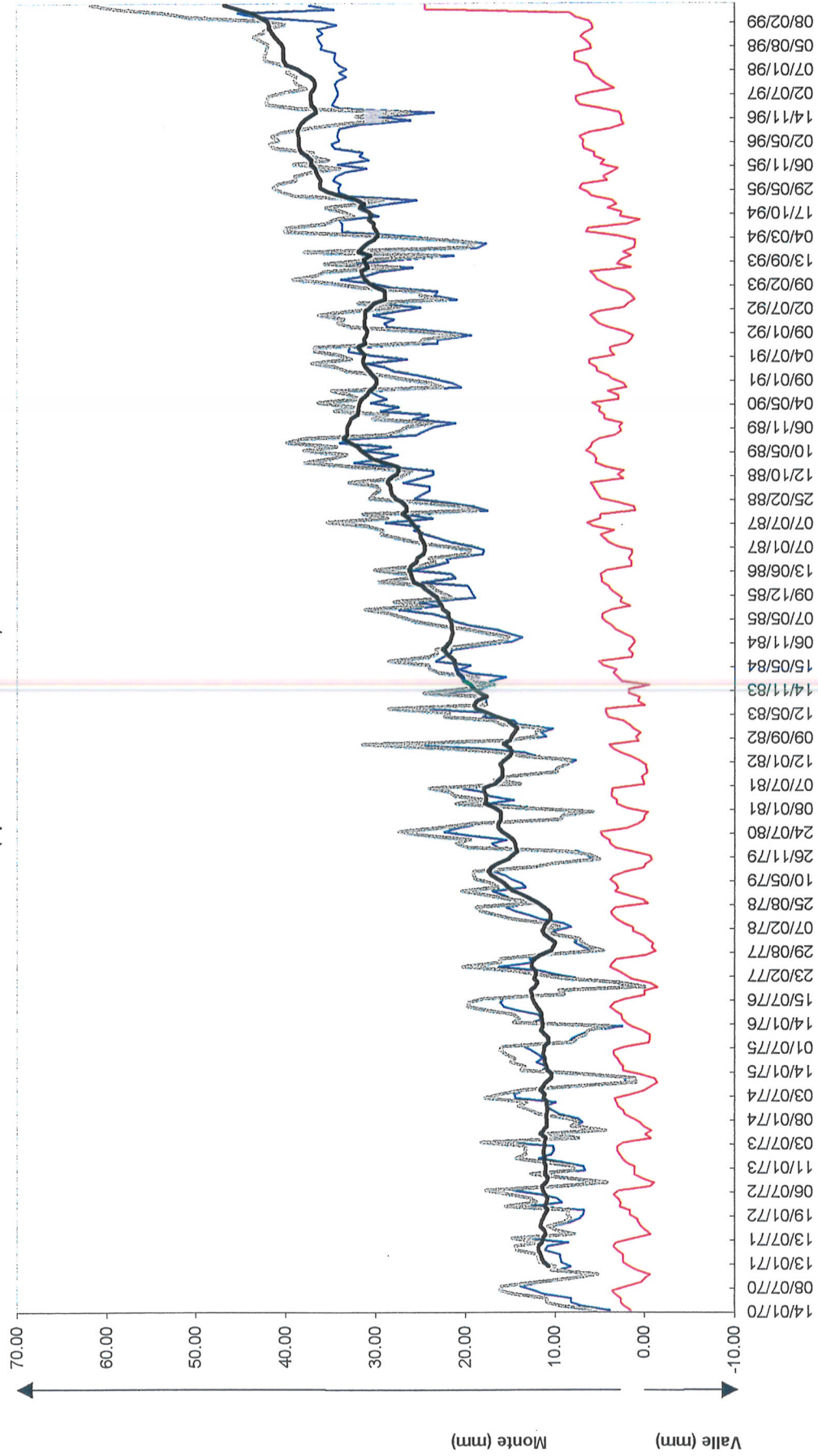
Diga Pianteleccio
Pendolo sponda destra (concio 18/20)
(Spostamenti monte / valle)



Diga Pianteleccio
Pendolo sponda destra (concio 18/20)
(Spostamenti destra / sinistra)

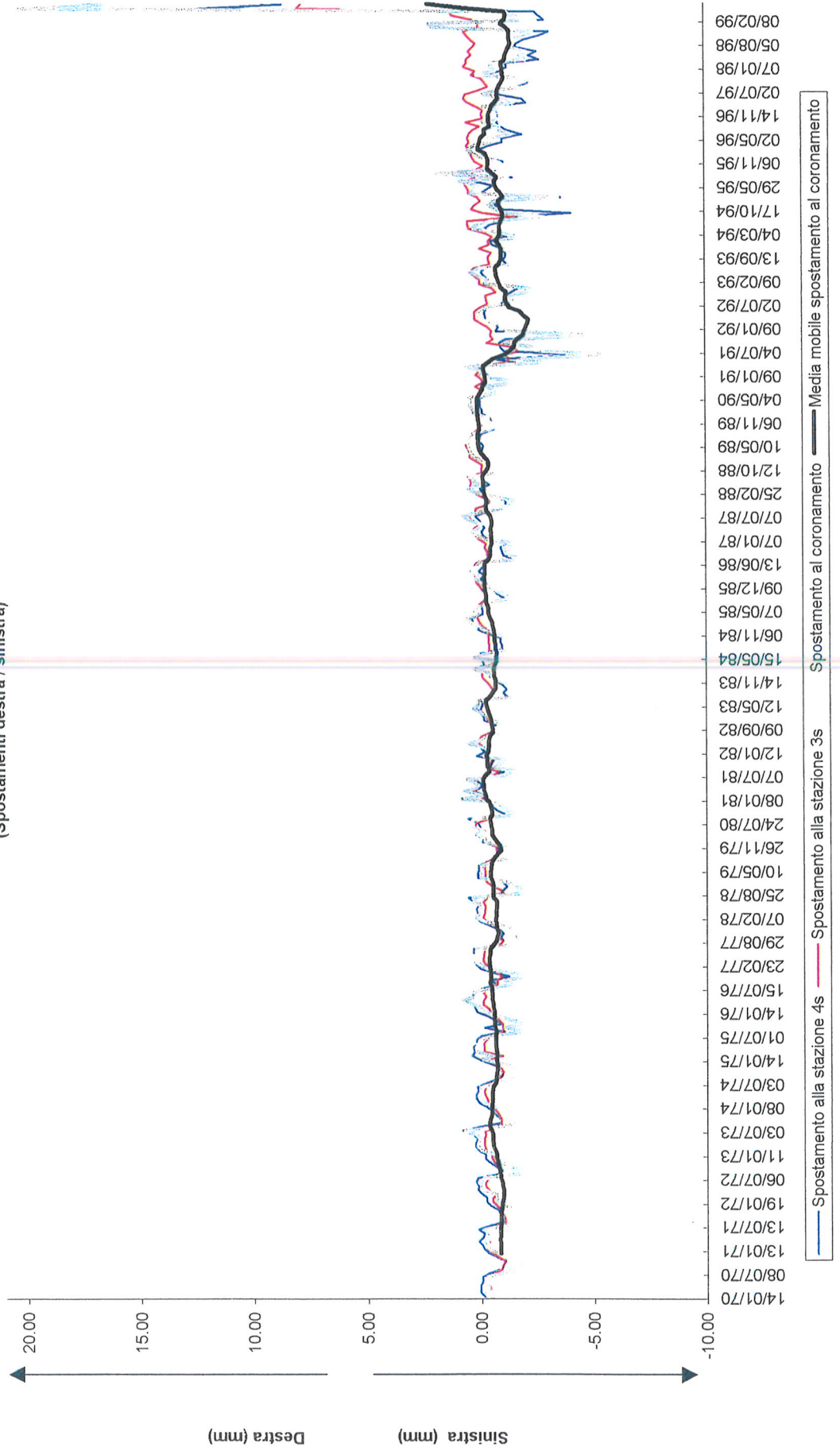


Diga Pianteleccio
Pendolo sponda sinistra (concio 11/13)
(Spostamenti monte / valle)



— Spostamento alla stazione 4s — Spostamento alla stazione 3s — Media mobile spostamento al coronamento

Diga Pianteleccio
Pendolo sponda sinistra (concio 11/13)
(Spostamenti destra / sinistra)



A. Popovici, R. Sarghiuta, A. Abdulamit, C. Ilinca
Forecast on stress-strain state generated by Alkali-Aggregate Reaction (AAR) from Pian
Telesio Dam

E. Bon, F. Chille, P. Masarati, C. Massaro

Analysis of the effects induced by alkali-aggregate reaction (AAR) on the structural behavior of Pian Telesio dam

FORECAST ON STRESS-STRAIN STATE GENERATED BY ALKALI-AGGREGATE REACTION (AAR) FROM PIAN TELESSIO DAM

A. POPOVICI, R. SÂRGIHUTA, A. ABDULAMIT, C. ILINCA
Technical University of Civil Engineering of Bucharest, ROMANIA

ABSTRACT. The prognosis at time 1999 and 2020 of some nodal displacements and stresses generated at Pian Telessio arch gravity dam ($H=80$ m) by Alkali-Aggregate Reaction (AAR) is presented in the paper. Using some monitoring data between 1970...1999 concerning reservoir water elevation, daily mean air temperatures, pendulums displacements, the effect of AAR on radial crest displacement is evaluated by statistical analysis with CONDOR model. The AAR time effect on dam stress-strain state is equivalated by uniform and linear increase of the dam body temperatures. The analysis is carried out in the dam-foundation system discretized in finite elements, provided by the formulator of the problem (ENEL Hydro-Polo Idraulico e Strutturale, Italy). The ANSYS computer code was applied in order to evaluate the required displacements and stresses.

1. INTRODUCTION

Pian Telessio dam is an arch-gravity structure ($H_{\max}=80$ m) from North-West of Italy commissioned in 1958 (Fig. 1). The dam had a normal behaviour until the middle of 1970 year.

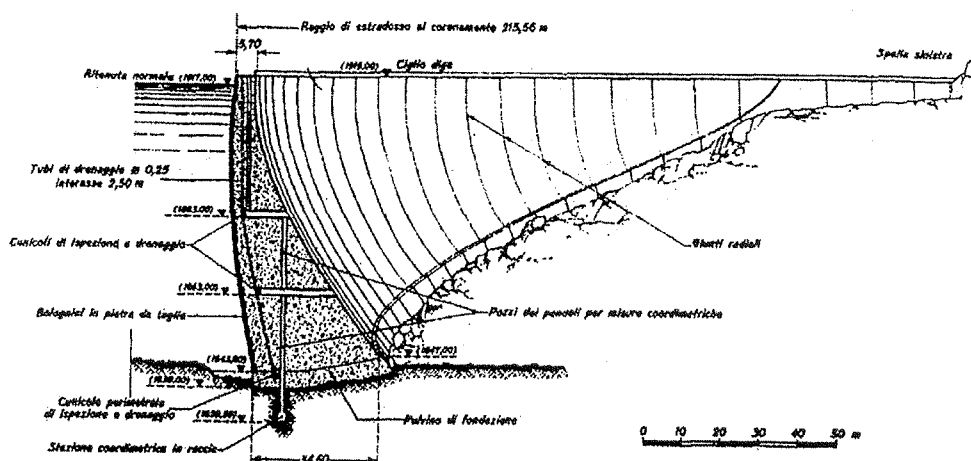


Figure 1. Pian Telessio Dam main cross section.

Soon after 1970 year, the measurements and other investigations (physical-chemical analyses) have clearly pointed out the development of AAR (Alkali-Aggregate Reaction) phenomenon.

Some prognoses about dam behaviour in the future pointing out the effects of AAR was decided to be one of the themes for VI-th International Benchmark Workshop on Numerical Analysis of Dams, Salzburg-2001. The formulator of the problem (ENEL Hydro-Polo Idraulico e Strutturale) provided the input necessary data (monitoring data, dam-foundation finite element mesh, material parameters, etc) in order to perform the prognosis about dam behaviour in the future. In this way the required output data are some displacements and stresses at time 1999 and 2020 in a number of selected nodes.

In the paper, the problem is solved in two steps. In the first step the contribution of AAR at the time history of the upstream-downstream crest displacements recorded by central pendulum is evaluated by statistical analysis using CONDOR model. In the second the AAR effect in time on dam stress-strain state is equivalated by uniform and linear increase of the dam body temperatures. The forecast of displacements and stresses until 2020 year is performed by structural analysis of a dam-foundation finite element mesh using ANSYS computer code.

2. STATISTICAL EVALUATION OF AAR EFFECTS ON RADIAL CREST DISPLACEMENTS IN THE CENTRAL CANTILEVER

The formulator provided the time history between 1970 and 1999 of the upstream-downstream crest displacements in the main cross section associated with reservoir water level and daily mean air temperature time histories.

Usually, the main parameters influencing the time variation of the dam displacements are air temperature and reservoir water level. However, in the case of Pian Telesio Dam the oscillogram of the radial crest displacement in the main cross section between 1970 and 1990 years, shows clearly every year a trend to upstream. This incessant swelling of the dam body is provoked, according to investigation results, by Alkali-Aggregate Reaction (AAR) phenomenon.

The statistical models, as is known, may be applied in order to separate the contribution of reservoir water level, air temperature and structure ageing (in this case AAR effect) on the dam displacements (Popovici, 2001).

In this paper, CONDOR model is applied in order to separate the contribution of the above mentioned factors on the radial crest displacements in the main cross section of Pian Telesio Dam CONDOR statistical model was developed by Coyne & Bellier being an improved variant of an older one developed by Electricite de France (EdF) (Mazenot, 1978). The usual CONDOR model was adapted for this particular case neglecting some terms, in order to put clearly in evidence the AAR effect. It may be mentioned that were tested different CONDOR model variants, finally being selected the most performant in the analysed particular case, as is presented in the following.

● The influence of the hydrostatic pressure was expressed alternatively by a third and fourth degree polynomial function as follows:

$$f_1(h) = a_2 h + a_3 h^2 + a_4 h^3 + a_5 h^4 \quad (1)$$

where h is relative depth of the reservoir in ratio with its normal retention level and $a_2...a_4$ influence coefficients to be determined.

- The structure ageing influence (AAR effect) was represented by a time linear function, respectively:

$$f_2(T) = a_6 T \quad (2)$$

where $T = \frac{D_i - D_0}{365.25}$ (years) with D_0 - reference date of the model, D_i - data of the recording and a_5 - influence coefficient to be determined.

During analysis of the structure ageing influence, had been taken into account and other terms as $a_7 e^{-T}$ (damped evolution) and $a_8 T^2$ (accelerated evolution), but finally they were eliminated, having distorsional effects.

- The seasonal temperature influence was modeled by a trigonometric function having the following form:

$$f_3(s) = a_7 \cos(s) + a_8 \sin(s) + a_9 \sin^2(s) + a_{10} \sin(s) \cos(s) \quad (3)$$

where $s = 2\pi \frac{D_i - D_0}{365.25}$ (rad).

The final relation of the CONDOR model had the form:

$$y = a_1 + f_1(h) + f_2(T) + f_3(s) + \varepsilon \quad (4)$$

where y is response parameter to be computed (radial crest displacements in the central cross section), a_1 - influence coefficient and ε - approximation error of the model.

The input data (water level time history, data of the recording, daily mean air temperatures time history) for statistical evaluation of the dam radial crest displacements in the central cross section were considered in two variants: as current values and respectively as mean 12 (mobile average). Some results of the analysis are illustrated in the Figures 2...7.

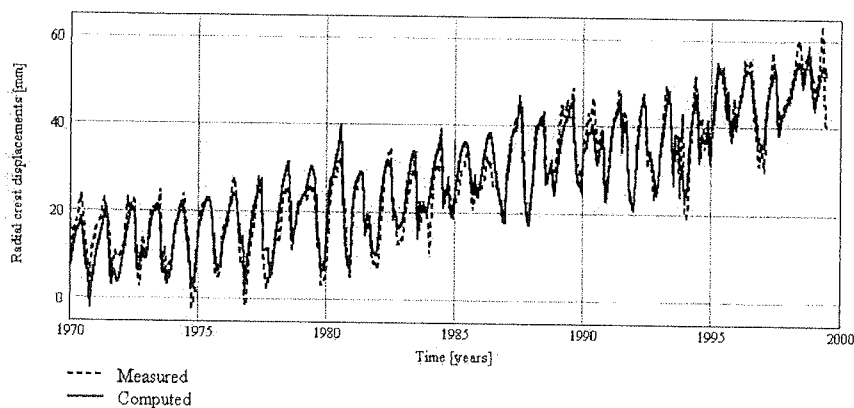


Figure 2. The time history of the radial crest displacements evaluated with CONDOR – variant 1 versus measured one.

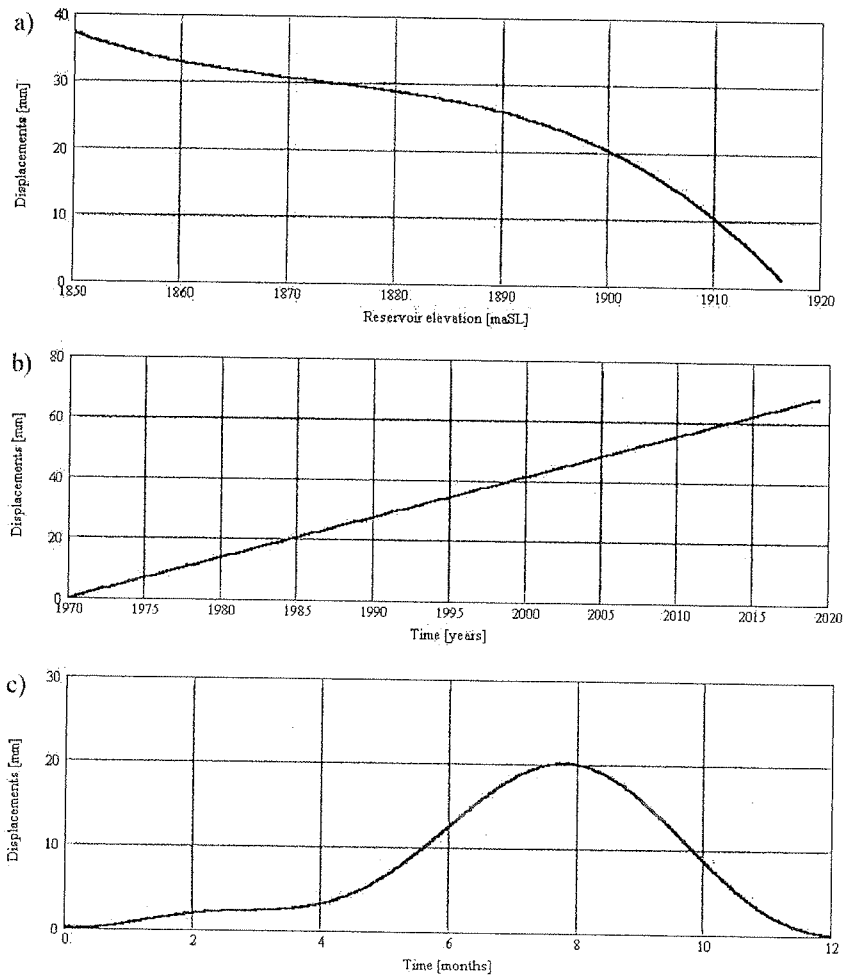


Figure 3. The influence of environmental factors on radial crest displacements computed with CONDOR - variant 1: a - hydrostatic level, b - AAR phenomenon, c - seasonal temperatures.

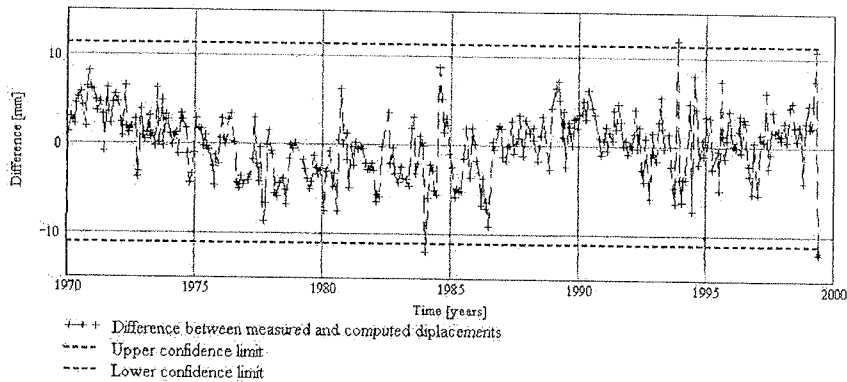


Figure 4. Differences between measured and computed values of the radial crest displacements with CONDOR - variant 1.

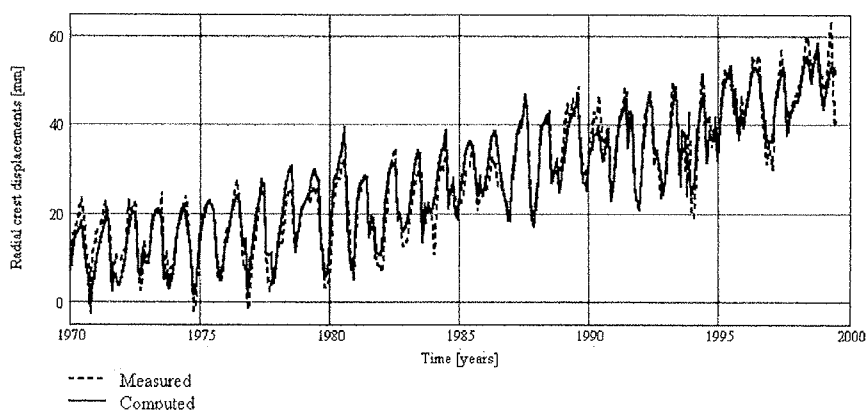


Figure 5. The time history of the radial crest displacements evaluated with CONDOR - variant 2 versus measured one.

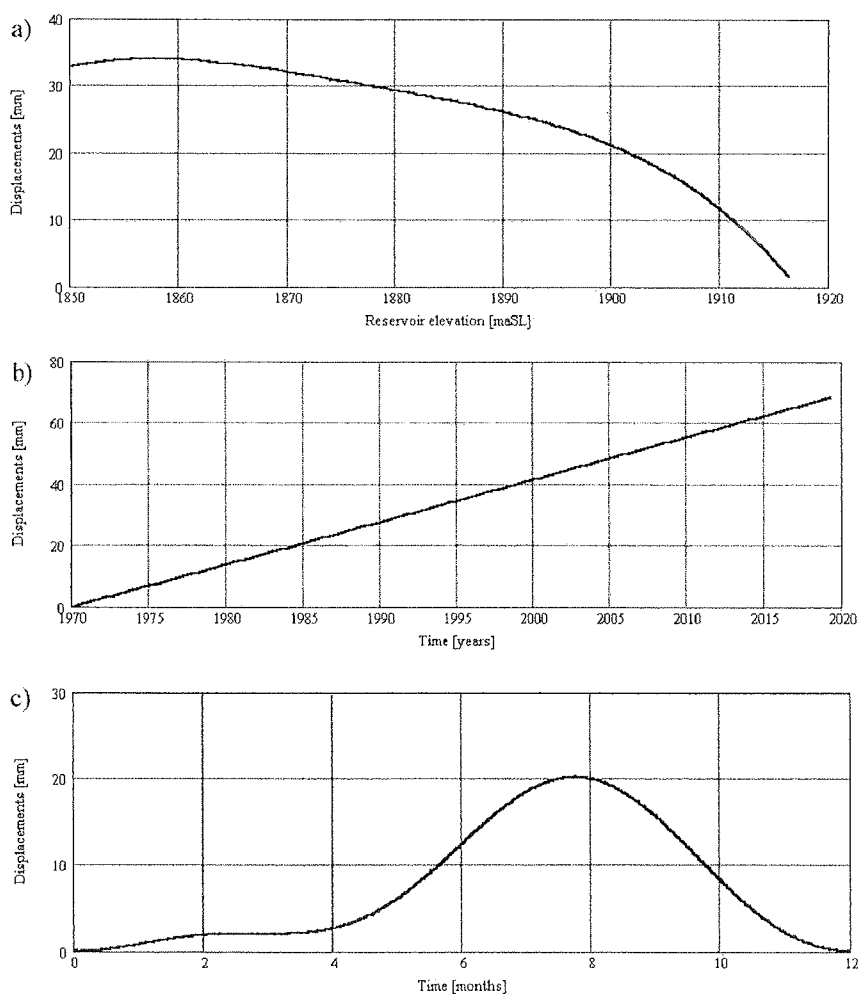


Figure 6. The influence of environmental factors on radial crest displacements computed with CONDOR - variant 2: a - hydrostatic level, b - AAR phenomenon, c - seasonal temperatures.

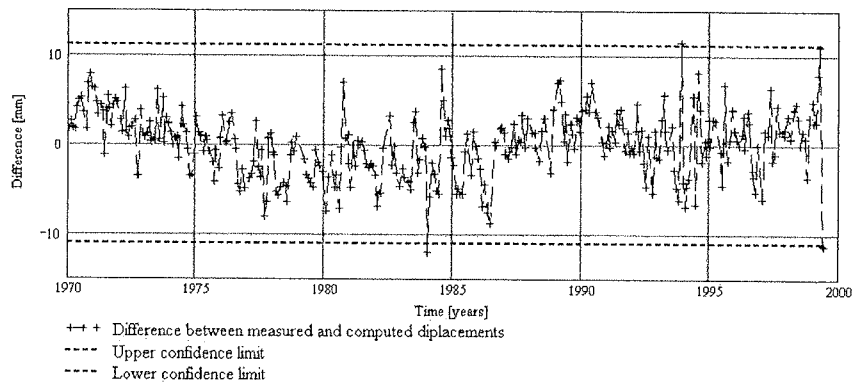


Figure 7. Differences between measured and computed values of the radial crest displacements with CONDOR - variant 2.

Concerning the results presented in the Figures 2...7 the followings must be specified:

CONDOR - variant 1 corresponds to a third degree polynomial function for modeling the hydrostatic pressure influence and current values for input data (environmental parameters);

CONDOR - variant 2 corresponds to a fourth degree polynomial function for modeling the hydrostatic pressure influence and current values for input data.

Based on comparative analysis between correspondent measured and computed values of the radial crest displacements, it may be concluded the both CONDOR variants reached good performances as accuracy degree. So, in CONDOR - variant 1, the limits of confidence for 98% Gauss probability reach ± 11.76 mm for the maximum amplitude of the measurements equal to 65.76 mm. In CONDOR - variant 2, the same limit of confidence reach ± 11.42 mm.

The global correlation ratios were $R = 0.966$ in CONDOR- variant 1 and respectively, the same value $R = 0.966$ in CONDOR- variant 2. Residual dispersions were $\sigma_{y,r} = 3.753$ in CONDOR - variant 1 and $\sigma_{y,r} = 3.714$ in CONDOR - variant 2.

The equations governing the radial crest displacements in the main cross section of Pian Telessio Dam (y), resulting by statistical analyses, have the following forms:

- CONDOR - variant 1

$$y = 32.69 - 83.55 h + 165.85 h^2 - 131.52 h^3 + \mathbf{1.385 T} - 6.29 \cos (s) - 6.79 \sin (s) + 2.78 \sin^2 (s) + 5.81 \sin (s) \cos (s) \quad (\text{mm}) \quad (5)$$

- CONDOR - variant 2

$$y = 9,62 + 112.14 h - 397.58 h^2 + 533.85 h^3 - 276.18 h^4 + \mathbf{1.387 T} - 6.27 \cos (s) - 6.83 \sin (s) + 2.57 \sin^2 (s) + 6.32 \sin (s) \cos (s) \quad (\text{mm}) \quad (6)$$

In compliance with relations (5) and (6) the AAR effects on radial crest displacements in the main cross section of Pian Telessio Dam (δ) may be expressed by the following relation:

$$\delta = 1.39 \mathbf{T} \quad (\text{mm}) \quad (+ \text{ to upstream}) \quad (7)$$

where \mathbf{T} is the number of years running since 1970.

Finally, by statistical analysis, it may be concluded that every year the AAR phenomenon generates a radial displacement to upstream of the Pian Telessio Dam crest in its main cross section equal to 1.39 mm. These displacements resulting by dam body swelling, may be equivalated by uniform increase of the dam body temperatures. This procedure will be presented at the following point.

3. FINITE ELEMENT ANALYSIS OF THE STRESS-STRAIN STATE GENERATED BY AAR

The finite element mesh suggested by formulator is illustrated in Figure 8. It is composed of 10427 nodes and 2044 elements and it was built according to ABAQUS computer code exigencies. The same parabolic brick (wedge) elements were used for discretizing dam body and foundation. Some parabolic quadrilateral interface elements were used to model the perimetral (pulvino) joint of the dam.

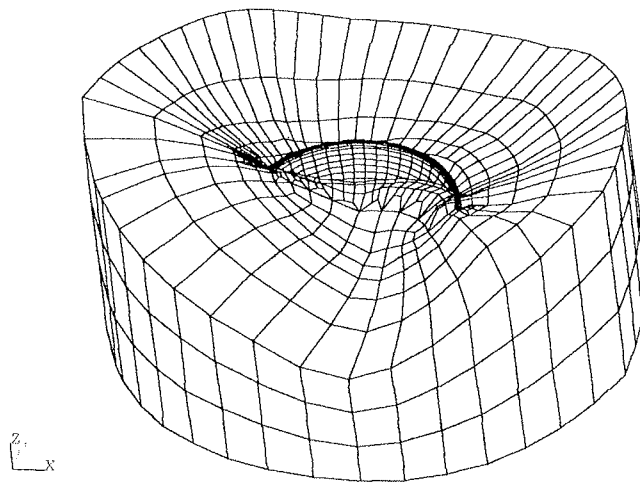


Figure 8. Finite element mesh of the dam-foundation system.

Some modifications in the finite element mesh above presented were made in order to be compatible with ANSYS computer code. So a number of very distorted elements from foundation were substituted. The interface elements from perimetral joint were also eliminated for simplifying of the problem and to transfer it in the linear elastic field.

The mechanical characteristics of the both dam concrete and foundation rock in function of load type are presented in Table 1. The finite element analysis was performed in the linear elastic field.

Table 1

	Load type	Young Modulus E [MPa]	Poisson ratio ν	Weight density [kN/m ³]
Concrete	dead weight, hydrostatic pressure	20.000	0.2	24.5
	A.A.R. effect	10.000	0.2	
	Rock foundation	28.000	0.2	-

The reduction of the E value at 0.5 of its current value for A.A.R. effect load is justified by the very slow time rate of this load. So, in a simplified manner is taken into account the concrete creep feature.

It was pointed out by finite element structural analysis that every year after 1970 the AAR phenomenon effect may be equivalated by an uniform increase of the dam body temperature with $1.07^0 C/year$ for a coefficient of thermal expansion $\alpha_t = 0.8 \times 10^{-5}$.

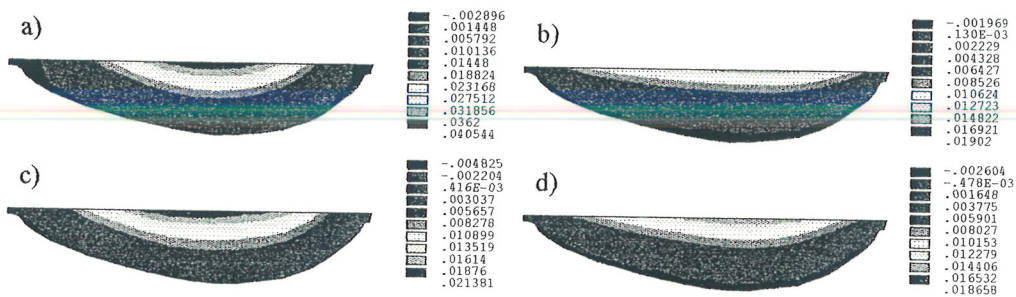


Figure 9. Pian Telessio Dam - Contours of the horizontal and vertical displacements [m] generated by AAR at 12/31/1999 (upstream face). a- horizontal upstream-downstream displacements due only to AAR; b-vertical displacements due only to AAR; c- total horizontal upstream-downstream displacements; d- total vertical displacements.

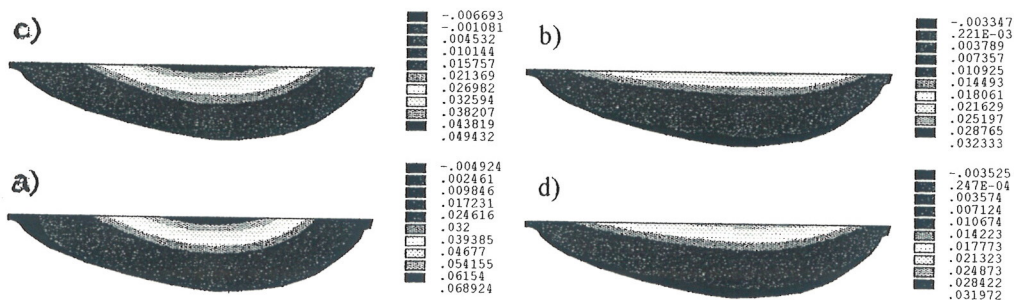


Figure 10. Pian Telessio Dam - Contours of the horizontal and vertical displacements [m] generated by AAR at 12/31/2020 (upstream face). a- horizontal upstream-downstream displacements due only to AAR; b-vertical displacements due only to AAR; c- total horizontal upstream-downstream displacements; d- total vertical displacements.

In the figures 9...16 are illustrated some results obtained by finite element analysis, concerning the AAR effects on the time stress-strain state at Pian Telessio Dam. The dead weight was applied only on the dam cantilevers. The reservoir was considered to be permanently placed at maximum storage level (1917 maSL). The AAR effect was taken into account according to relation (7).

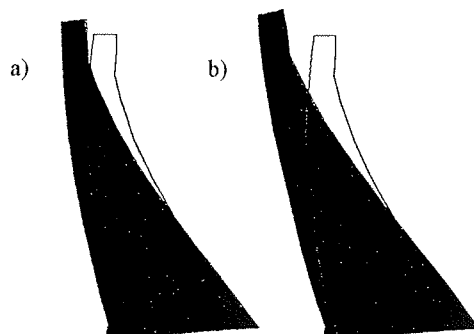


Figure 11. Displacements of the dam main cross section generated by AAR at 12/31/1999 and 12/31/2020.

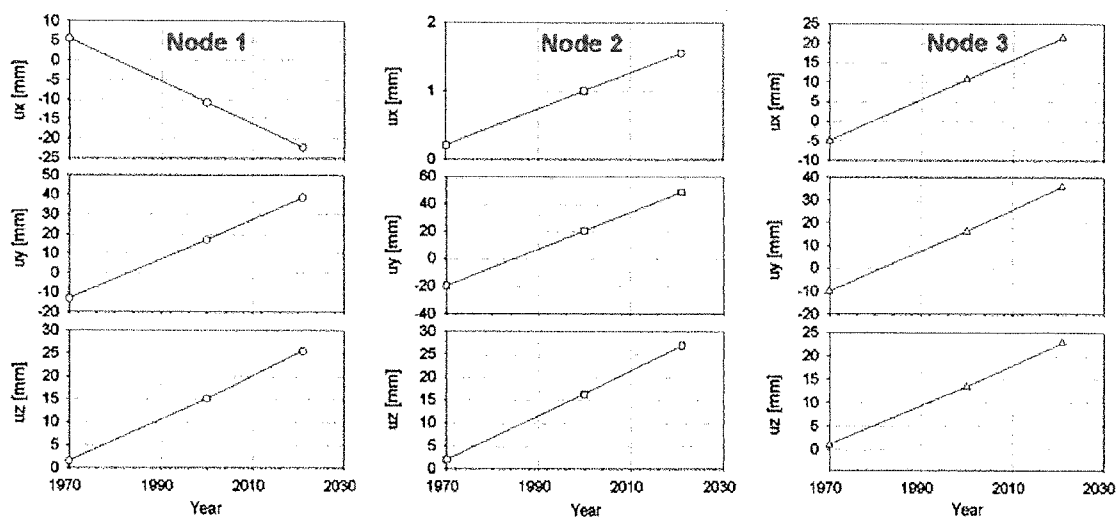


Figure 12. Time histories of the displacements generated by dead weight, hydrostatic pressure and AAR for three selected nodes from dam's crest.

The maximum horizontal displacements to upstream of the dam body because of AAR by swelling effect reach 4 cm at the end of 1999 year and respectively 6.9 cm at the end of 2020 year (Fig. 9 and Fig. 10). These results were confirmed also by statistical analysis (see Fig. 3 b and 6 b). Moreover, by finite element analysis, was put in evidence the increase of the dam height because of AAR. So, the maximum vertical displacements on up direction because of AAR reach 1.9 cm at the end of 1999 year and respectively 3.2 cm at the end of 2020 year. The rate of displacements increase is constant in time but differing from node to node according to initial hypothesis (Fig. 12).

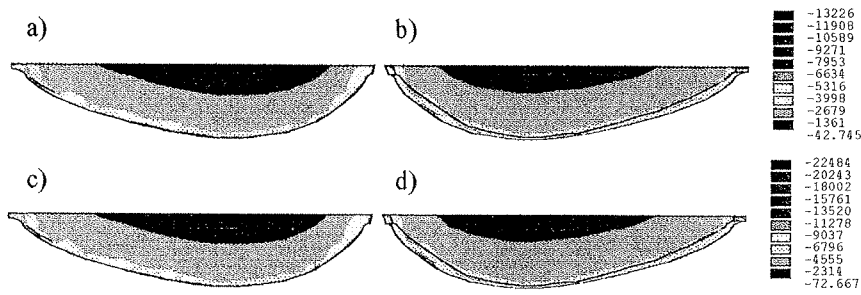


Figure 13. Pian Telessio Dam - Contours of the principal minimum stresses (σ_3) generated by AAR at 12/31/1999 (a, b) and 12/31/2020 (c, d). a, c- upstream face; b, d- downstream face.

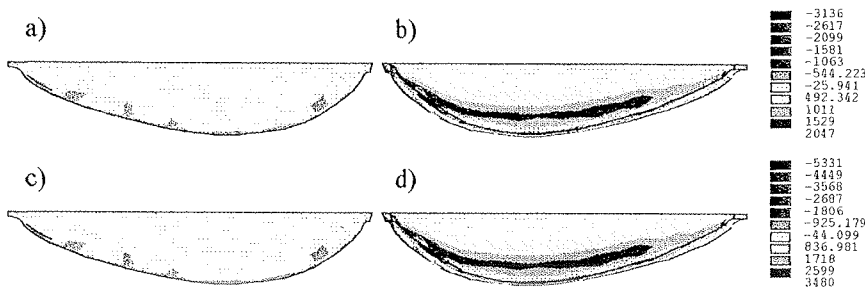


Figure 14. Pian Telessio Dam - Contours of the principal maximum stresses (σ_1) generated by AAR at 12/31/1999 (a, b) and 12/31/2020 (c, d). a, c- upstream face; b, d- downstream face.

The contours of the principal minimum and maximum stresses generated by AAR phenomenon at the end of 1999 and 2020 year can be seen in the Figures 13 and 14. The maximum compressive stresses only because of AAR reach - 6.63 MPa at the end of 1999 and - 11.27 MPa at the end of 2020 year. The maximum tensile stresses because of AAR reach 1.75 MPa at the end of 1999 and 2.90 MPa at the end of 2020 year.

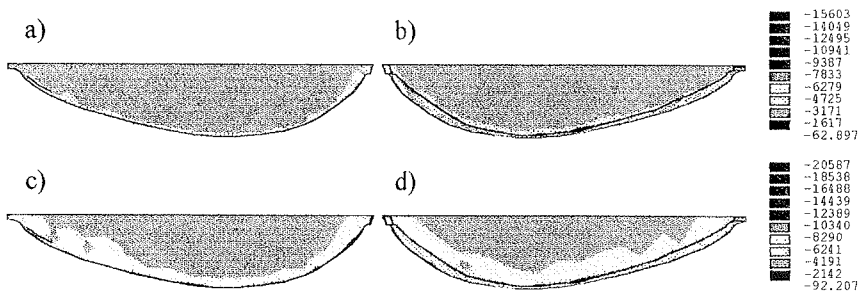


Figure 15. Pian Telessio Dam - Contours of the principal minimum stresses (σ_3) generated by dead weight+hydrostatic pressure (maximum reservoir level) + AAR at 12/31/1999 (a, b) and 12/31/2020 (c, d). a, c- upstream face; b, d- downstream face.

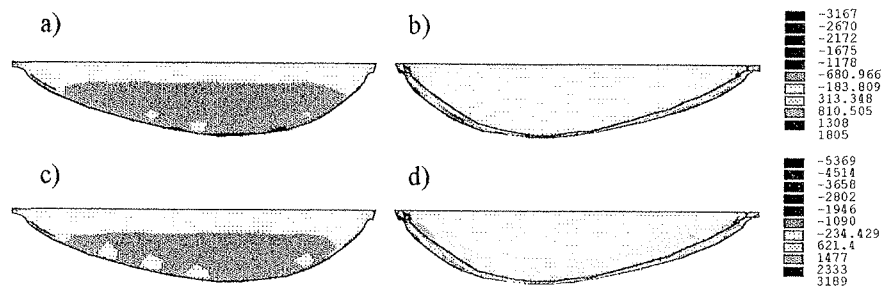


Figure16. Pian Telessio Dam - Contours of the principal maximum stresses (σ_1) generated by dead weight+hydrostatic pressure (maximum reservoir level) + AAR at 12/31/1999 (a, b) and 12/31/2020 (c, d). a, c- upstream face; b, d- downstream face.

The contours of the principal stresses generated by dead weight+hydrostatic pressures (corresponding to reservoir maximum level) + AAR at the end of 1999 and 2020 year are presented in the Figures 15 and 16. The maximum compressive stresses produced by the loads combination above mentioned reach -10.94 MPa at the end of 1999 and -16.49 MPa at the end of year 2020. In the same loads combination the maximum tensile stresses reach 1.31 MPa at the end of 1999 and 2.33 MPa at the end of 2020.

4. CONCLUDING REMARKS

The forecast on the time evolution of the stress-strain state provoked by Alkali-Aggregate Reaction (AAR) from Pian Telessio Dam was performed by finite element structural analysis. Firstly the AAR effect on dam displacements was assumed to be linear and was evaluated on the basis of some data from dam behaviour monitoring. Secondly, the AAR effect was equivalated by uniform and linear increase of the dam body temperature. So, taking into account a coefficient of thermal expansion $\alpha_t = 0.8 \times 10^{-5}$, the AAR effect could be equivalated by a constant rate of the increase of the dam body temperature of 1.07^0 C/year.

Based on finite element analysis, performed with ANSYS computer code, may be emphasized the following remarks:

- the dam body has displacements to upstream (horizontal direction) and to up (vertical direction) because of AAR; for instance at the end of 2020 year the maximum displacements of the dam crest in the central section reach 6.9 cm to upstream and 3.2 cm to up;
- the stress state generated by AAR is important; at the end of 2020 year the maximum compressive stresses only because of AAR reach -11.27 MPa and maximum tensile stresses reach 2.9 MPa.
- the stresses generated by loads combination of dead weight + hydrostatic pressures + AAR reach the following maximum values: compressive stresses at the end of 1999 -10.94 MPa and, respectively at the end of 2020 -16.49 MPa; tensile stresses at the end of 1999 1.31 MPa and respectively at the end of 2020 2.33 MPa.

The behaviour of the concrete and rock materials from dam-foundation system was modeled as linear elastic one.

REFERENCES

- ICOLD 2001, VI-th Benchmark Workshop on Numerical Analysis of Dams. Theme A - Evaluation of Alkali - Aggregate Reaction effects on the structural behaviour of an arch dam ENEL-HYDRO-Polo Idraulico e Strutturale.
- Popovici, A. 2001 Dams for water storage. Second volume. (in Romanian) (under press).
- Mazenot, P. 1978. Methode generale d'interpretation des mesures de surveillance des barrages en exploitation a Electricite de France. EDF - Division Technique Generale.